Dinitroacetylene: Can It be Made?

Citation for the original published paper (version of record):
Harter, L., Bélanger-Chabot, G., Rahm, M. (2025). Dinitroacetylene: Can It be Made?. Propellants, Explosives, Pyrotechnics, 50(4). http://dx.doi.org/10.1002/prep.12019

Propellants, Explosives, Pyrotechnics

WILEY-VCH

Propellants, Explosives, Pyrotechnics

RESEARCH ARTICLE OPEN ACCESS

Dinitroacetylene: Can It be Made?

Lara Harter[1] | Guillaume Bélanger-Chabot[1] | Martin Rahm[2]

[1]Department of Chemistry, Centre de Recherche sur les Matériaux Avancés (CERMA) and Centre en chimie verte et catalyse, Université Laval, Quebec, Canada | [2]Department of Chemistry and Chemical Engineering, Chalmers University of Technology, Gothenburg, Sweden

Correspondence: Guillaume Bélanger-Chabot (gbchabot@chm.ulaval.ca) | Martin Rahm (martin.rahm@chalmers.se)

Keywords: alkynes | energetic materials | kinetic stability | nitrite | nitro compounds

ABSTRACT

With a predicted record-high heat of formation, energy density, and outstanding performance as a rocket propellant, dinitroacetylene stretches the imagination for what is possible in terms of organic chemical explosives and monopropellants. In this study, we employ quantum chemical methods to predict its thermodynamic properties, ionization potential, electron affinity, ultraviolet-visible spectra, nuclear magnetic resonance, and vibrational spectra, and to investigate proposed decomposition mechanisms. While unimolecular decomposition pathways are predicted to have high activation energies, nitrogen oxide radical species—commonly present in reaction mixtures of energetic materials—are found to significantly catalyze the decomposition of dinitroacetylene. This catalytic effect may explain previous unsuccessful synthesis attempts. A frontier orbital analysis suggests that partial reduction could increase the C—N bond order, offering a strategy to stabilize this elusive high-energy-density material.

1 | Introduction

In this work, we computationally evaluate dinitroacetylene (**1**) as a possible future high-energy density material (HEDM). Development [1] of improved HEDMs is a challenging task motivated by both a military and civilian need for explosives and propellants and growing environmental concerns [2]. Industry workhorses such as the secondary explosive RDX, and the oxidizer ammonium perchlorate are associated with detrimental environmental persistence and significant toxicity. The development of new energetic materials is challenging in part due to the need for a higher energy content, which typically results in lower kinetic stability. This delicate balance has historically led to diminishing returns [3]. Figure 1 shows a selection of state-of-the-art explosives and more recent HEDMs, alongside one important metric for their energy content, the energy density, that is, energy released upon self-combustion.

While the design of energetic materials is a complex multifaceted process, the energy density represents a particularly important parameter that can be optimized for. Small-molecule monopropellants are particularly good examples of extremes in energetic content [4]. One inspiration for our work is nitryl cyanide ($NCNO_2$)[1m], a material that, despite being kinetically persistent at ambient conditions, carries an estimated energy density of 2 kcal/g. As such, $NCNO_2$ is an ultra-high energy density material, outclassing even the infamously sensitive hydrogen azide (ca. 1.6 kcal/g) [5]. Nitryl cyanide reaches close to the theoretical limit of energy density for a single-component carbon-based energetic material because it is designed to carry a perfect oxygen balance. In other words, its stoichiometry, in principle, allows for complete decomposition into CO_2 and N_2.

Dinitroacetylene (**1**), the conceptual product of double nitration of acetylene, is one of the few hypothetical molecules that could potentially exceed the energy density of nitryl cyanide. Like $NCNO_2$, dinitroacetylene is also perfectly oxygen-balanced—its complete decomposition creates two equivalents of CO_2. Early work by Shechter et al. predicted a high positive heat of formation of 89 kcal/mol (HF/6-31G*) for **1** [6]. As we shall see, this value is in fair agreement with our revised estimates.

Nitroacetylene (**2**) and some of its derivatives O_2N—CC—R (R = trimethylsilyl, tert-butyl, iodo, etc.) have been synthesized

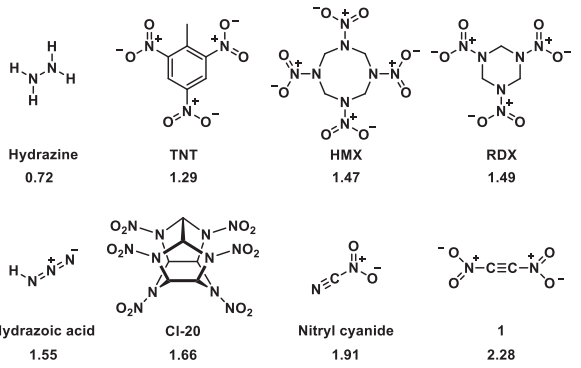

FIGURE 1 | Energy density of selected energetic materials in their standard state in kcal/g. TNT = trinitrotoluene; HMX = octogen or 1,3,5,7-tetranitro-1,3,5,7-tetrazocine; RDX = hexogen or 1,3,5-trinitro-1,3,5-triazinane; Cl-20 = hexanitrohexaazaisowurtzitane. Energy densities are based on idealized reactions, see ESI for further details.

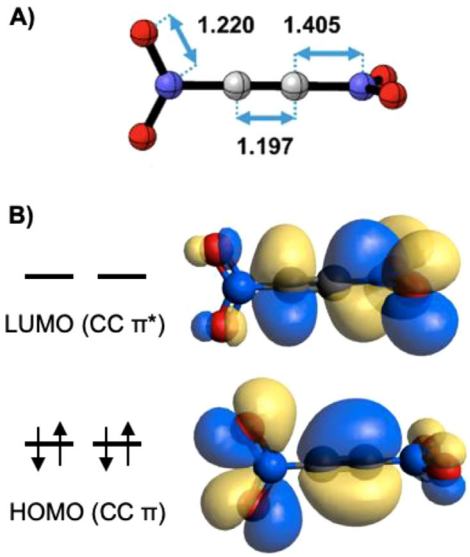

FIGURE 2 | (A) Geometry of **1** predicted at the B3LYP/6-311G(d,p) level of theory. (B) Highest occupied molecular orbital (HOMO) and the lowest occupied molecular orbital (LUMO) orbitals of **1**, where both are of *E* symmetry and represent a degenerate pair.

and isolated [7]. A review detailing the challenges (and many failures) of the synthesis of nitroacetylenes and **1** has been published by Vollhard et al. [7]. Such attempts include dehydrohalogenation reactions on 1,2-dinitroethylene derivatives, reverse cycloadditions of acetylenedicarboxylate with 2,5-dibromo-3,4-dinitrothiophene followed by pyrolysis [8], and various nitration conditions on acetylene derivatives. Examples of the latter include introducing acetylene gas to fuming nitric acid [7], and reactions between various nitrating agents, such as NO_2BF_4 and N_2O_4, and phenylacetylides. These same nitrating agents and reaction conditions have also been applied to nitro(trimethylsilyl)acetylene without success, as mild conditions did not yield any conversion, while harsher conditions directly led to decomposition products [7].

The elusiveness of **1** has motivated several computational studies on the reactivity and decomposition mechanisms of **1**. Alster et al. noted that because the thermal decomposition of nitromethane occurs via a nitrite intermediate, the decomposition of **1** might happen via its nitrite isomer [9]. They predicted a three-membered ring intramolecular isomerization mechanism with a corresponding activation enthalpy of 20 kcal/mol using the semi-empirical MINDO/3 method [7, 9, 10]. The nitrite isomer is subsequently presumed to undergo thermolysis to generate NO or NO_2 radicals [7]. Until present, this mechanism has been the best explanation for the instability of **1**.

Politzer and co-workers have used HF/6-31G level of theory calculations to predict that the two NO_2 groups of **1** are oriented perpendicular to one another with the planar structure being disfavored by 0.8 kcal/mol [6, 11]. Estimates of the electrostatic surface potential have also showed **1** to be highly electron-deficient and therefore insensitive to electrophilic attack [11]. Jursic have used B3LYP/6-31G(d)//AM1 calculations to predict that **1** can react with furan via a cycloaddition reaction that is thermodynamically favorable with an activation barrier of ca. 8 kcal/mol [12]. Wiener and co-workers predicted the possibility for highly exergonic formation of octanitrocubane from **1** through a series of cyclooligomerization steps at the B3P86/6-31G** level [13]. These predictions have shown that **1** is not only a potential energetic material but also a powerful synthon for other intriguing energetic molecules.

Computational method accuracy has developed substantially since these earlier predictions on **1** and its properties [6, 9, 11–13]. In what follows, we outline revised thermodynamic and kinetic stability estimates of **1**, and we propose plausible decomposition pathways alongside strategies for its detection and stabilization.

2 | Results and Discussion

2.1 | Structure of Dinitroacetylene and a Strategy for Its Stabilization

Figure 2A shows our predicted structure of **1** in the gas phase. The molecule is D_{2d}-symmetric with one nitro group twisted by 90°. The reason for the twisted structure is not sterics, but electronics. Prior work has suggested that this configuration is adopted because it permits the NO_2 group to conjugate with one of the π-bonds of the carbon–carbon triple bond, producing an additional stabilization of the system [6, 11].

The electronic structure of **1** is noteworthy because both its highest occupied molecular orbital (HOMO) and the lowest occupied molecular orbital (LUMO) are of the same symmetry, *E* (Figure 2B). The *E*-representation (which is doubly degenerate) of the D_{2d} point group allows significant mixing of the frontier orbitals. One way to rationalize this unique electronic structure is by the combination of a CC π/π^* fragment with two symmetry-adapted NO_2 π/π^* fragment orbitals (not shown).

The resulting HOMO orbital(s) shown in Figure 2 correspond to two central CC π-bonds, each twisted by 90° relative to two sets of N—O π-bonds, which in turn are turned 90° with respect to each other. Conversely, the two degenerate lowest unoccupied molecular orbitals (LUMO) each correspond to two C—N π-bonding interactions, one set on each side of the molecule, and a C—C anti-bonding interaction.

Because C—N bonds are often the weakest link (*trigger bond*) of nitro compounds, the orbital topology of **1** suggests to us a possible route to its stabilization. Reduction of **1**, that is, occupation or partial occupation of the LUMO should strengthen the molecule's weakest link, at the cost of weakening its strongest. We will return to discuss the evaluation of this hypothesis after discussing the inherent energy density and reactivity of **1**.

2.2 | The Energy Content of Dinitroacetylene

We have used a topological analysis of the electrostatic surface potential (see the methods section) to estimate enthalpies of vaporization and sublimation, $\Delta H_{vap} \approx$ 8.3 and $\Delta H_{sub} \approx$ 11.8 kcal/mol. From these values, we can infer that **1** is likely a gas, possibly a volatile liquid, at ambient conditions. We make this inference by comparison to the structurally related molecule $NCNO_2$, which has an experimentally determined ΔH_{vap} of 6.8 ± 0.2 kcal/mol, and an extrapolated boiling point of 7°C.[1m] Our computational approach is also validated by comparison to $NCNO_2$, whose predicted value for ΔH_{vap} is 6.7 kcal/mol, only 0.1 kcal/mol different from experiment.

Our best estimate of the heat of formation of **1** in the gas phase, $\Delta H^0_{f(1,gas)}$ is 85.0 ± 2 kcal/mol. This value was estimated from the most recent $\Delta H^0_f - NIST$ data (NIST = National Institute of Standards and Technology) for CO_2 (−94.1 kcal/mol) [14], combined with a CBS–QB3 (extrapolated CCSD(T), see methods section) reaction enthalpy for [Equation (1)] of ΔH°_r = −273.2 kcal/mol:

$$\mathbf{1} \xrightarrow{\Delta H^\circ_r} 2CO_2(-94.1) + N_2(0.0) \quad (1)$$

Our estimate for $\Delta H^0_{f(1,gas)}$ is considerably more reliable compared to previous estimates at the Hartree-Fock level of theory [7], which range between 89 and 52 kcal/mol [6, 15].

The heat of formation of **1** in its liquid state can be estimated from our calculation of ΔH_{vap} as $\Delta H^0_{f(1,liquid)}$ = 85.0–8.3 = 76.7 kcal/mol. Such a high enthalpy of formation is, to our knowledge, unprecedented for small molecules. Not only does it far exceed that of known monopropellants and conventional explosives (Table S1), but it also largely explains why **1** has eluded successful synthesis. Our calculated energy for complete decomposition of **1** corresponds to an energy density of 2.28 kcal/g in the condensed phase, which surpasses even nitryl cyanide, arguably the most energetic molecule still kinetically persistent at ambient conditions (Figure 1)[1m].

In terms of rocket propellant performance, the energy content we predict for **1** corresponds to a specific impulse of 354 s. This is an exceedingly high value for a monopropellant, where relevant comparisons are 343 s (predicted) for nitryl cyanide and 239 s (predicted) for a state-of-the-art hydrazine propellant.

2.3 | Unimolecular Decomposition of 1

Figure 3 summarizes studied pathways for the unimolecular decomposition of **1**, both in the gas phase and from a model accounting for solvation effects by acetonitrile. Our prediction for the homolytic dissociation enthalpy of the C—N bond is ~80 kcal/mol, nearly independent of the environment, a value sufficiently large to preclude such a process as a realistic decomposition pathway at ambient conditions. Note that we use relative enthalpies as our estimate of all dissociation barriers and not the relative free Gibbs energy. We do so because the entropic gain associated with an increased number of rotational and translational degrees of freedom upon dissociation is only fully realized after the bond is broken. The relative enthalpy of the separated fragments therefore represents an upper estimate of the real Gibbs free energy barrier [16]. Heterolytic bond dissociation is, as expected, considerably less feasible in the gas phase. However, dissociation of NO_2^+ becomes comparable to the homolytic route in solution, with an enthalpy cost of ca. 76 kcal/mol.

Nitro (—NO_2) ↔ nitrite (—ONO) isomerization into nitroethynyl nitrite (**3**) or ethyne-1,2-diyl dinitrite (**4**) is calculated as more plausible routes to unimolecular decomposition of **1**. Our barrier estimates for the first (into **3**) and second isomerization (into **4**) are, in solution: 49.7 kcal/mol and 59.1 kcal/mol, respectively. These values are in stark contrast to the 20 kcal/mol value predicted in 1984 by Alster et al. [7, 9]. We attribute the large difference to the lower semi-empirical level of theory in the earlier work. As reference, we remind here that for a first-order reaction to proceed at meaningful time scales near ambient conditions, its barrier needs to be below ca. 30 kcal/mol. In other words, our predicted barrier height shows conclusively that **1** cannot decompose through **TS1 and TS2** near ambient conditions but can do so at higher temperatures.

While **3** has a planar geometry, **4** carries its nitrite groups at a dihedral angle of ca. 93° in the gas phase. As shown in Figure 3, **3** and **4** are both weakly associated complexes of significantly (~15 kcal/mol) lower energy than **1**. This is in stark contrast with the usual nitro/nitrite ordering, which finds nitroalkanes usually more stable than their nitroalkanes counterparts. While **3** can be thought of as two weakly bound O_2NCCO and NO radicals, **4** is a complex between O═C═C═O (a triplet ground state) and two NO radicals. These complexes are both higher in energy than their fully dissociated states. The dissociation of NO fragments from **3** and **4** is nearly barrierless and spontaneous: we estimate the bond dissociation Gibbs free energy of **3** to −9.5 kcal/mol, while for **4**, dissociation into two NO molecules and O═C═C═O is thermodynamically downhill by −38.5 kcal/mol in the gas phase (the values are not much different in solution, c.f., Figure 3). Further dissociation of O═C═C═O into two CO molecules can proceed following cross-over to the close-lying singlet state [17]. The kinetic instability of the nitrito-isomers is again in stark contrast with nitritoalkanes, many of which are commercially available, like amyl nitrite. However, for such isomers to offer a potential explanation to the elusiveness of **1**, their formation must proceed through a different route than TS1.

2.4 | Decomposition of 1 via Nitrogen Oxide-Catalysis

The most likely route to the decomposition of **1** that we have identified involves catalysis by nitrogen oxide (NO_x) radical species (Figure 4), which are frequently found as side-products in

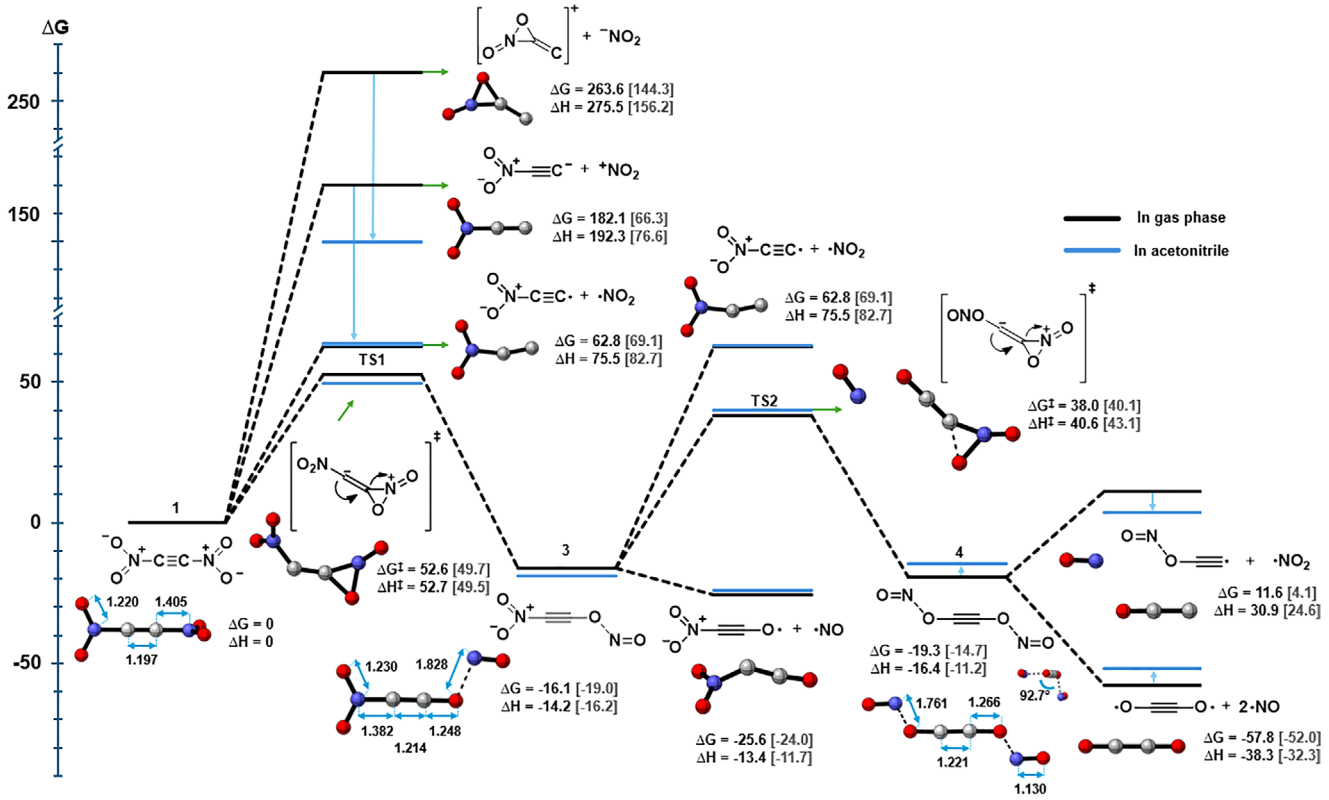

FIGURE 3 | Studied unimolecular decomposition routes for **1**. Relative Gibbs energies and enthalpies in kcal/mol are provided for the gas phase in black. Predicted values in acetonitrile solution are provided in gray within brackets and are indicated by blue arrows and lines. Bond lengths for selected gas-phase structures are shown in Ångström.

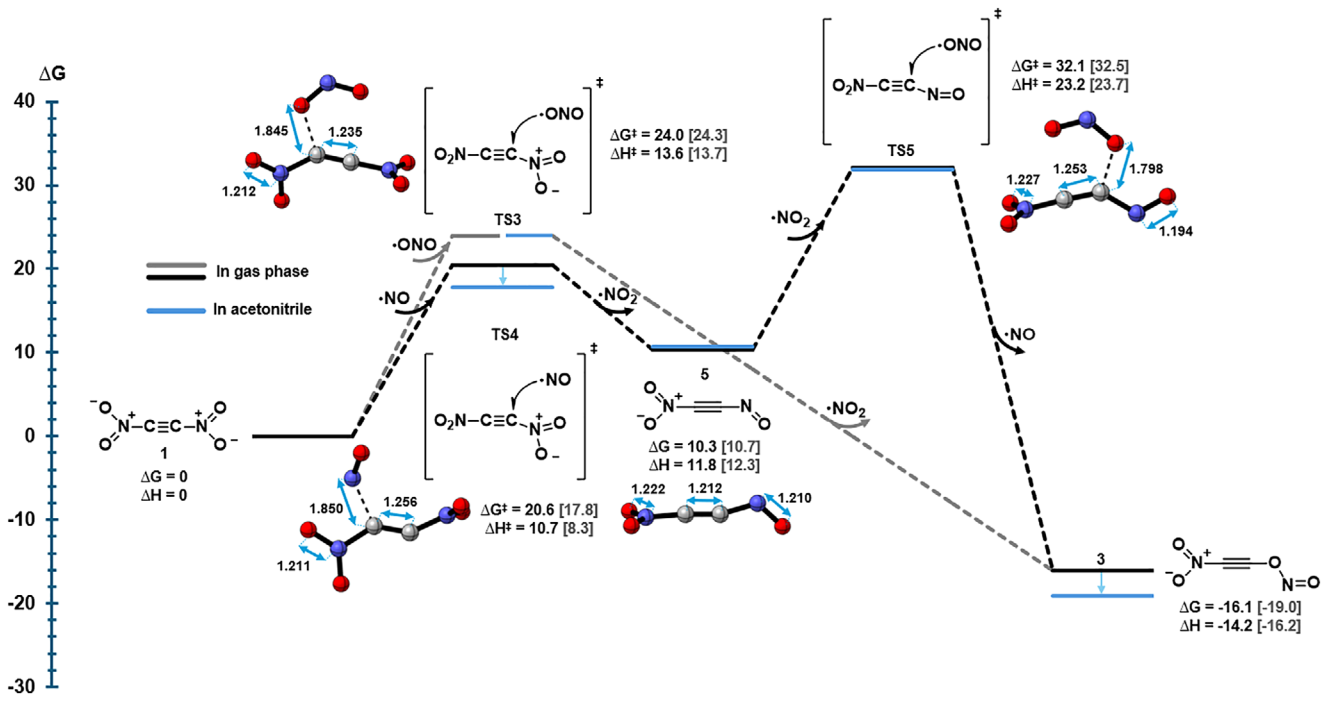

FIGURE 4 | Proposed routes to decomposition of **1** via nitrogen-oxide-mediated nitro/nitrite isomerization. The NO_2-mediated pathway is depicted with gray lines, while the NO-mediated pathway is depicted with black lines. Relative Gibbs energies and enthalpies in kcal/mol are provided for the gas phase in black. Predicted values in acetonitrile solution are provided within brackets and are indicated by blue arrows and lines. Selected bond lengths in gas-phase structures are shown in Ångström.

reaction mixtures related to energetic materials. We predict NO_2-mediated nitro-nitrite isomerization to be highly accessible, with a Gibbs free energy barrier of 24.3 kcal/mol in solution (Figure 4). Because we have established that the resulting nitrite isomer **3** can rapidly decompose (c.f., Figure 3), this overall mechanism can allow rapid and complete decomposition of **1** well below room temperature.

NO is also able to react with **1** over an estimated Gibbs free energy barrier of only 17.8 kcal/mol in solution. The formation of the resulting intermediate 1-nitro-2-nitrosoacetylene (**5**) is, however, thermodynamically unfavorable by ∽10 kcal/mol. Compound **5** has rather strong C—N bonds and is likely to be more kinetically persistent than **3** and **4**. However, the reaction of **5** with NO_2 is nonetheless predicted to be nearly accessible at ambient conditions, with a Gibbs free energy barrier of ca. 32.1 kcal/mol, and exergonic by ca. 30 kcal/mol in solution. We can speculate that also other radical species are likely able to act as decomposition catalysts of **1.**

2.5 | Detection Characteristics

Due to its propensity for NO_x-catalyzed decomposition, any observation of **1** is likely to be done spectroscopically at low temperatures. To aid such efforts, we have predicted the vibrational spectrum of **1** (see Table S2) and its ^{14}N chemical shift (δ = −96.6 ppm with respect to nitromethane). We also note that despite the same symmetry (*E*) of the frontier orbitals, electronic transitions between them are allowed under the symmetry selection rules of the D_{2d} point group. However, allowed in principle need not mean allowed in practice. An equation-of-motion coupled cluster calculation predicts the first excited states to be a degenerate set of triplets (of B_2 and B_1 symmetry) 3.44 eV (360 nm) above the ground state, which, alongside the third and fourth lowest excited state, is inaccessible due to spin symmetry. What is more surprising is that transitions into the manifold of lowest-lying singlet states similarly all correspond to zero (or very near zero) oscillator strengths. We attribute this prediction to a plentitude of oppositely polarized degenerate levels resulting in net cancellations of transition dipoles. Only the 15^{th} lowest excited state (out of singlets and triplets), at approximately 6.5 eV (190 nm) above the ground state, boasts an appreciable oscillator strength (Figure S1). In other words, while **1** is unlikely to persist in the presence of trace amounts of NO_x, the molecule does appear to be quite photostable.

2.6 | Can Dinitroacetylene be Stabilized by Reduction?

With the relative instability of **1** established, we look next to our previously hypothesized route to stabilization by reduction. We estimate in vacuo ionization potential (IP) and electron affinity (EA) of **1** to 11.5 and 2.6 eV, respectively. The latter value is large (60 kcal/mol) and nearly matches that of Buckminsterfullerene, C_{60} ! Dinitroacetylene is so electrophilic, in fact, that even the double reduction is thermodynamically allowed in vacuum (by 0.5 eV or 12 kcal/mol). Our thermodynamic estimates for capture of electrons solvated by acetonitrile are approximate (see methods section for details) but indicate substantial spontaneity of 3.0 and 2.6 eV (69 and 58 kcal/mol), for the first and second reduction, respectively. In other words, both the radical anion ($\mathbf{1}^{\bullet-}$) and dianion ($\mathbf{1}^{2-}$) of **1**, should be thermodynamically stable in solution with respect to oxidation. However, as shown in Figure S6, $\mathbf{1}^{2-}$ is thermodynamically unstable with respect to (near barrierless) heterolytic ejection of a nitrite anion and will not be considered further.

The radical anion $\mathbf{1}^{\bullet-}$ will, of course, be highly reactive. We study its structure and behavior in isolation in what follows for it can be a first model for understanding how **1** might act as a coordinating ligand (Figure 5). In contrast to **1**, we predict the radical anion ($\mathbf{1}^{\bullet-}$) to be planar, with D_{2h} symmetry in the gas phase and in solution.

As we can expect from our frontier orbital analysis, the C—N bonds in gas-phase $\mathbf{1}^{\bullet-}$ (1.348 Å) are computed as shorter compared to those in **1** (1.405 Å). The C—C bonds are also lengthened by reduction, to 1.219 Å in $\mathbf{1}^{\bullet-}$ compared to 1.197 Å in **1**. The reduction is accompanied by a predicted marginal red shift in the C—N and C—C vibrational frequencies of ∼24 cm^{-1} (Tables S2 and S3, ESI). We note that this slight decrease in C—N frequency for the shorter C—N bond contradicts Badger's rule. The lower frequency is, however, reflected in the C—N bond dissociation enthalpies in $\mathbf{1}^{\bullet-}$, which we predict to be ΔH_{diss} = 21.4 kcal/mol for the homolytic dissociation in solution (Figure 5), much lower than that for **1** (ΔH_{diss} = 82.7 kcal/mol, Figure 3).

As we have emphasized, the radical anion of **1** is but a first model approximation to studying the potential for stabilization through reduction. Important steps towards the realization of such a strategy have already been made by Vollhardt and coworkers, who successfully synthesized nitroacetylene [18] adducts with cobalt(0). We intend to return in future work to explore the use of transition metal coordination to facilitate the stabilization of **1** in practice.

3 | Conclusion

Dinitroacetylene (**1**) would, if made, carry an energy density unparalleled in existing chemical explosives. Our quantum chemical analysis has provided revised estimates for its heat of formation, spontaneity, and barrier to decomposition. One likely pathway for its decomposition under reaction conditions is revealed to be NO_x-catalyzed nitro-nitrite isomerization. Frontier orbital rationales combined with an exceedingly high predicted electron affinity for **1** are used to suggest reduction, possibly through metal coordination, as a stabilizing mechanism. A look at $\mathbf{1}^{\bullet-}$ indicates a C—N bond shortening as a result of reduction, however, the associated bond dissociation enthalpy is lowered compared to neutral **1**.

The great oxidizing character of **1** coupled with its high reactivity and low kinetic stability indicates that isolating **1** would be a formidable experimental challenge. Our work, in concert with that of Vollhardt et al., suggests that organometallic chemistry may offer pathways for catching a glimpse of this elusive molecule. However, if made, possible applications of the compound will likely be limited to use as an energetic synthetic intermediate.

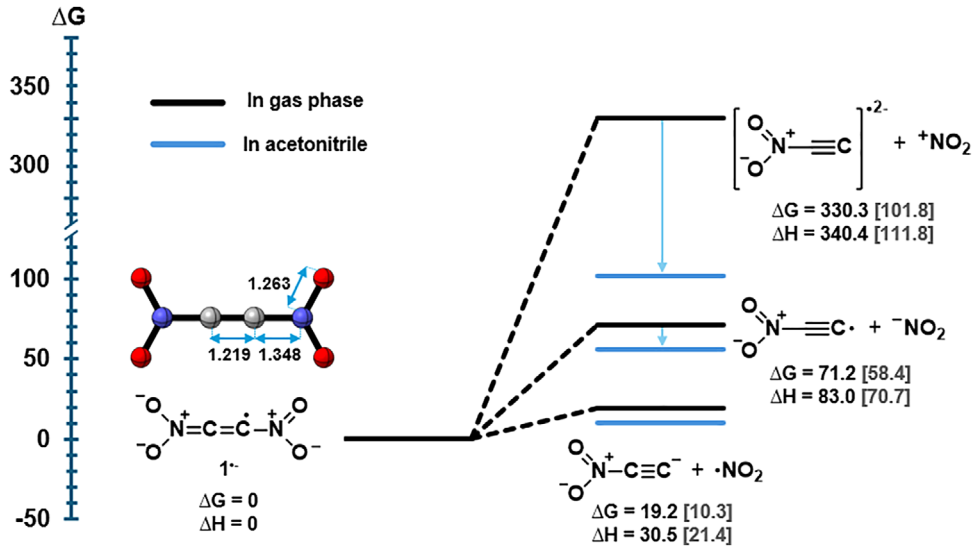

FIGURE 5 | Homolytic and heterolytic dissociation energies for $\mathbf{1}^{\bullet-}$ in kcal/mol. Relative Gibbs energies and enthalpies in kcal/mol are provided for the gas phase in black. Predicted values in acetonitrile solution are provided in gray within brackets and are indicated by blue arrows and lines. Bond lengths for the gas-phase structure are shown in Ångström.

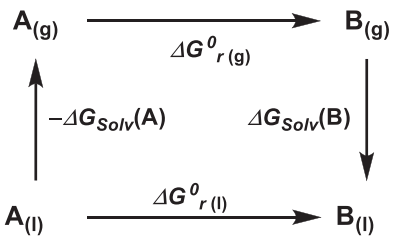

FIGURE 6 | Thermodynamic cycle used for calculating relative free energies in acetonitrile.

4 | Methodology

All calculations have been performed using Gaussian 16, revision C.01 [19]. Modeling of **1** and its derivatives in the gas phase have been performed using the composite CBS-QB3 method [20], known to yield accurate energies for small organic molecules and radical species [21]. The basis of CBS-QB3 is a coupled cluster (CCSD(T)) calculation, which is extrapolated to the basis-set limit using MP2 and MP4 energies and empirical corrections. Geometries and thermodynamic corrections are in the CBS-QB3 method obtained at the B3LYP/6-311G(d,p) level of theory.

To estimate Gibbs free energies of reaction and activation in acetonitrile (ΔG^0_{CH3CN}), we utilize a thermodynamic cycle outlined in Figure 6.

In this approach, we correct our CBS-QB3 gas-phase energies using solvation energies calculated separately using density functional theory combined with the implicit SMD [22] model. The solvation energy by CH_3CN for a species A is defined as:

$$\Delta G_{\text{solv}}(A) = G_{CH_3CN}(A) - G_{\text{gas-phase}}(A), \tag{2}$$

where $G_{CH3CN}(A)$ and $G_{\text{gas-phase}}(A)$ are total Gibbs free energies estimated following geometry optimization and frequency analysis at the M06-2X [23]/aug-cc-pVTZ level of theory, with and without SMD modeling of acetonitrile, respectively. Final relative Gibbs free energies are provided for a 1 M and 298 K standard state and are calculated for a reaction step A → B as:

$$\Delta G^0_{CH_3CN} = \Delta G^0_{\text{gas-phase}}(CBS-QB3) + \Delta G_{\text{solv}}(B) - \Delta G_{\text{solv}}(A) \tag{3}$$

Reaction enthalpies in solution are estimated following Equation (3), but with $\Delta G^0_{\text{gas-phase}}$ replaced by $\Delta H^0_{\text{gas-phase}}$.

Electron capture of **1** in acetonitrile solution is estimated by Equation (3) combined with approximate solvation energy for the electron by acetonitrile of −31.7 kcal/mol. This theoretical value has been derived from SMD+B3LYP/aug-cc-pVTZ calculations by Marković et al. [24].

ΔH_{vap} and ΔH_{sub} of **1** is estimated from the electrostatic surface potential calculated at the B3PW91/6-31G(d) level using a parametrized relationship [25] and the HS95 (version EAUHF) program [26].

The 30 lowest singlet and triplet excitations are calculated for the ground state geometry of **1** at the EOM-CCSD/aug-cc-pVTZ level of theory [27].

Rocket performance calculations were performed with the RPA software version 2.3.2, using a chamber pressure of 7 MPa and an expansion area ratio of 70.

Acknowledgments

G. Bélanger-Chabot acknowledges the Natural Sciences and Engineering Research Council of Canada (NSERC) for an Alliance-Catalyst grant. This research relied on computational resources provided by the National Academic Infrastructure for Supercomputing in Sweden (NAISS) at C3SE and NSC partially funded by the Swedish Research Council through

grant agreement No. 2022-06725. This research was also enabled in part by support provided by Calcul Québec (www.calculquebec.ca) and the Digital Research Alliance of Canada (www.alliancecan.ca). The authors also thank Professors Denis Boudreau and Frédéric-Georges Fontaine for fruitful discussions.

Data Availability Statement

The data that support the findings of this study are openly available on the Borealis repository at: https://doi.org/10.5683/SP3/HM2I9A.

References

1. a) I. Gospodinov, K. V. Domasevitch, C. C. Unger, M. Benz, J. Stierstorfer, and T. M. Klapötke, "Energetic Derivatives of 3,3′,5,5′-tetranitro-4,4′-bipyrazole (TNBPz): Synthesis, Characterization and Properties," *FirePhysChem* 4 (2024): 1–9. b) J. Yount, M. Morris, N. Henson, M. Zeller, E. F. C. Byrd, and D. G. Piercey, "Sequential, Electrochemical-Photochemical Synthesis of 1,2,4-Triazolo-[4,3-a]pyrazines," *Chemistry—A European Journal* 30, no. 2 (2024): e202400661. c) J. P. Agrawal, *High Energy Materials* (Weinheim: Wiley-VCH Verlag GmbH & Co. KGaA, 2010). d) D. S. Viswanath, T. K. Ghosh, and V. M. Boddu, *Emerging Energetic Materials: Synthesis, Physicochemical, and Detonation Properties* (Dordrecht: Springer Netherlands, 2018). e) A. K. Yadav, M. Jujam, V. D. Ghule, and S. Dharavath, "High-performing, Insensitive and Thermally Stable Energetic Materials from Zwitterionic Gem -dinitromethyl Substituted C–C Bonded 1,2,4-Triazole and 1,3,4-Oxadiazole," *Chemical Communications* 59 (2023): 4324–4327. f) C. Lei, H. Yang, W. Yang, Q. Zhang, and G. Cheng, "Synthesis of Ideal Energetic Materials with High Density and Performance Based on 5-Aminotetrazole," *Crystal Growth & Design* 22 (2022): 2594–2601. g) S. Liao, T. Liu, Z. Zhou, K. Wang, S. Song, and Q. Zhang, "Energetic Isomers of Bridged Oxadiazole Nitramines: The Effect of Asymmetric Heterocyclics on Stability and Energetic Properties," *Dalton Transactions* 50 (2021): 13286–13293. h) Y. Wang, L. Hu, S. Pang, and J. n. M. Shreeve, "Nitroimino as an Energetic Group in Designing Energetic Materials for Practical Use, a Tautomerism from Nitroamino," *Journal of Materials Chemistry A* 11 (2023): 13876–13888. i) A. K. Chinnam, R. J. Staples, and J. n. M. Shreeve, "Bisnitramide-Bridged N-Substituted Tetrazoles with Balanced Sensitivity and High Performance," *Organic Letters* 25 (2023): 1481–1485. j) K. Pandey, A. Tiwari, J. Singh, et al., "Pushing the Limit of Oxygen Balance on a Benzofuroxan Framework: K 2 DNDP as an Extremely Dense and Thermally Stable Material as a Substitute for Lead Azide," *Organic Letters* 26 (2024): 1952–1958. k) S. Lal, R. J. Staples, and J. n. M. Shreeve, "Design and Synthesis of High-Performance Planar Explosives and Solid Propellants with Tetrazole Moieties," *Organic Letters* 25 (2023): 5100–5104. l) R. Haiges and K. O. Christe, "5-(Fluorodinitromethyl)-2 H-Tetrazole and Its Tetrazolates—Preparation and Characterization of New High Energy Compounds," *Dalton Transactions* 44 (2015): 10166–10176. m) M. Rahm, G. Bélanger-Chabot, R. Haiges, and K. O. Christe, "Nitryl Cyanide, $NCNO_2$," *Angewandte Chemie International Edition* 53 (2014): 6893–6897.

2. a) K. Panz and K. Miksch, "Phytoremediation of Explosives (TNT, RDX, HMX) by Wild-type and Transgenic Plants," *Journal of Environmental Management* 2012, 113, 85–92. b) L. E. Braverman, X. He, S. Pino, et al., "The Effect of Perchlorate, Thiocyanate, and Nitrate on Thyroid Function in Workers Exposed to Perchlorate Long-Term," *Journal of Clinical Endocrinology and Metabolism* 90 (2005): 700–706.

3. T. M. Klapötke, *Chemistry of High-energy Materials* (Berlin: de Gruyter, 2012).

4. G. Bélanger-Chabot, M. Rahm, R. Haiges, and K. O. Christe, "Ammonia–(Dinitramido)boranes: High-Energy-Density Materials," *Angewandte Chemie International Edition* 2015, 54, 11730–11734.

5. a) B. Ruscic, Active Thermochemical Tables (ATcT) Values Based on ver. 1.118 of the Thermochemical Network, (2015). b) B. Ruscic, R. E. Pinzon, M. L. Morton, et al., "Introduction to Active Thermochemical Tables: Several "Key" Enthalpies of Formation Revisited," *Journal of Physical Chemistry A* 108, (2004): 9979–9997.

6. P. Politzer, P. Lane, P. Sjoberg, M. E. Grice, and H. Shechter, "Calculated Structures and Heats of Formation of Some Predicted C, N, O, F Molecules," *Structural Chemistry* 6, (1995): 217–223.

7. G. K. Windler, P. F. Pagoria, and K. P. C. Vollhardt, "Nitroalkynes: A Unique Class of Energetic Materials," *Synthesis* 2014, 46, 2383–2412.

8. M. J. S. Dewar, Dinitroacetylene and Related Compounds, Government Report ADA128954, US Government; Research Triangle Park (NC, USA): (1983).

9. M. J. S. Dewar, J. P. Ritchie, and J. Alster, "Ground States of Molecules. 65. Thermolysis of Molecules Containing NO2 Groups," *Journal of Organic Chemistry* 50, (1985): 1031–1036.

10. D. F. V. Lewis, "MINDO/3: A Review of the Literature," *Chemical Reviews* 86, (1986): 1111–1123.

11. P. Politzer and R. Bar-Adon, "Electrostatic Potentials and Relative Bond Strengths of Some Nitro- and Nitrosoacetylene Derivatives," *Journal of the American Chemical Society* 109,(1987): 3529–3534.

12. B. S. Jursic, "The Inertia Principle and Implementation in the Cycloaddition Reaction With Aromatic Heterocycles Performed With AM1 Semiempirical and Density Functional Theory Study," *Journal of Molecular Structure: Theochem* 459, (1999): 215–220.

13. P. L. Politzer, P. Wiener, and J. John, Defense Technical Information Center, (1999).

14. J. D. Cox, D. D. Wagman, and V. A. Medvedev, CODATA Key Values for Thermodynamics, Hemisphere Publishing Corp., New York, (1984).

15. A. V. Golovin and V. V. Takhistov, "Thermochemistry of Organic and Heteroorganic Species. Part XII. Mono- and Disubstituted Acetylenes and Ethynyl Free Radicals. New Electronegativity Scale," *Journal of Molecular Structure* 701, (2004): 57–91.

16. G. Bélanger-Chabot, M. Rahm, R. Haiges, and K. O. Christe, "$[BH_3C(NO_2)_3]^-$: The First Room-Temperature Stable (Trinitromethyl)Borate," *Angewandte Chemie International Edition* 52, (2013): 11002–11006.

17. D. Schröder, C. Heinemann, H. Schwarz, J. N. Harvey, S. Dua, S. J. Blanksby, and J. H. Bowie, "Ethylenedione: An Intrinsically Short-Lived Molecule," *Chemistry-A European Journal* 4, (1998): 2550–2557.

18. M.-X. Zhang, P. E. Eaton, I. Steele, and R. Gilardi, "Nitroacetylene: $HC{\equiv}CNO_2$," *Synthesis* 14, (2002): 2013–2018.

19. M. J. Frisch, G. W. Trucks, H. B. Schlegel, et al., 16 Rev. C.01 (Wallingford, CT: GaussView 5.0., 2016).

20. J. A. Montgomery Jr., M. J. Frisch, J. W. Ochterski, and G. A. Petersson, "A Complete Basis Set Model Chemistry. VI. Use of Density Functional Geometries and Frequencies," *Journal of Chemical Physics* 110, (1999): 2822–2827.

21. B. Sirjean, R. Fournet, P.-A. Glaude, and M. F. Ruiz-López, "Extension of the Composite CBS-QB3 Method to Singlet Diradical Calculations," *Chemical Physics Letters* 435, (2007): 152–156.

22. A. V. Marenich, C. J. Cramer, and D. G. Truhlar, "Universal Solvation Model Based on Solute Electron Density and on a Continuum Model of the Solvent Defined by the Bulk Dielectric Constant and Atomic Surface Tensions," *Journal of Physical Chemistry B* 113, (2009): 6378–6396.

23. Y. Zhao and D. G. Truhlar, "The M06 Suite of Density Functionals for Main Group Thermochemistry, Thermochemical Kinetics, Noncovalent Interactions, Excited States, and Transition Elements: Two New Functionals and Systematic Testing of Four M06-class Functionals and 12 Other Functionals," *Theoretical Chemistry Accounts* 120, (2008): 215–241.

24. Z. Marković, J. Tošović, D. Milenković, and S. Marković, "Revisiting the Solvation Enthalpies and Free Energies of the Proton and Electron in Various Solvents," *Computational & Theoretical Chemistry* 1077, (2016): 11–17.

25. P. Politzer, Y. Ma, P. Lane, and M. C. Concha, "Computational Prediction of Standard Gas, Liquid, and Solid-Phase Heats of Formation

and Heats of Vaporization and Sublimation," *Int J Quant Chem* 105, (2005): 341–347.

26. a) T. Brinck, Hardsurf program (HS95vEAUHF) (2015). b) T. Brinck and J. H. Stenlid, "The Molecular Surface Property Approach: A Guide to Chemical Interactions in Chemistry, Medicine, and Material Science," *Advanced Theory and Simulations* 2, (2019): 1800149.

27. J. F. Stanton and R. J. Bartlett, "The Equation of Motion Coupled-Cluster Method. A Systematic Biorthogonal Approach to Molecular Excitation Energies, Transition Probabilities, and Excited State Properties," *Journal of Chemical Physics* 98, (1993): 7029–7039.

Supporting Information

Additional supporting information can be found online in the Supporting Information section.